Flow Numerical Analysis for Selecting the Best Arrangements of Apartment Buildings

Sajad Armand,
Technical and Vocational Institute of Sama, Islamic Azad University, Unit of West Islam Abad, Kermanshah, Iran
Master of Science in Mechanical Engineering (Energy Conversion), Lecturer at University, Member of the Engineering Council of Kermanshah, address: building 56, Madrese Alley, Amir Abad, West Islam Abad, Kermanshah, Iran
Behrouz Armand,
Bachelor of Civil Engineering (Civil Engineering), Islamic Azad University of Kermanshah, Address: building 20, Mina Alley, west Islam Abad, Kermanshah, Iran
Mohsen Armand
Associate degree in civil Engineering (civil), Islamic Azad University of Islam Abad, Address: building 23, Hassan Khan Alley, 700 Dastgah, west Islam Abad, Kermanshah, Iran

Abstract

In this study two-dimensional and calm flow numerical solution on two warm Cylinders with constant temperature with rectangular cross-section located inside a canal with insulator walls have been studied. The problem for blockage ratio of 0.125, distance between the barriers equal to 1 to 4 times of the height of the barriers and Reynolds numbers in the range of 100 to 300 have been conducted. The effect of change in each of the parameters on Nusselt number, level of heat transfer, drag and lift coefficients and Coefficient of friction and the effect of distance changes between the barrier to canal wall on level of heat transfer and also the effect of changes in Reynolds number on these coefficient have been studies. The governing equations have been solved with the use of discretized finite volume method and the obtained Algebraic equations and for solving Navier-Stokes equations A semi-implicit fractional step method has been used. Values of drag coefficient and average Nusselt number have been calculated for four different grids and have been compared with each other and finally, the appropriate grid has been selected .Increased Reynolds number in blockage ratio of 0.125 for the 1st barrier in all the S/Hs leads to increased drag coefficient. However, for the 2nd barrier and in S/H=1 and S/H=2, drag coefficient decreases. In S/H=3 and S/H=4, considering the change of flow shape and the fact that the space between the two barriers are not filled with vortices, until the Reynolds number in which the space between the barriers are filled, drag coefficient decreases and then after than increases. This critical Reynolds in S/H=3 is 250 and it is 150 in S/H=4. With increasing the distance between the barriers in blockage ratio of 0.125, for the 1st barrier, average Nusselt increases, however, increased Reynolds number has a direct effect on increasing average Nusselt in different distances of barriers. The highest jump in average Nusselt in different Reynolds is seen in the barrier distance between 3H and 4H which is due to Vortex shedding phenomenon in heat transfer. On the 2nd barrier also, increased distance between barriers in general leads to increased average Nusselt in which Reynolds number has a direct relationship with increased average Nusselt.

Keywords: *numerical analysis, Navier-Stokes, Reynolds, calm flow, critical Reynolds*

Introduction

The flow on barriers inside a canal has attracted the attention of many researchers in different fields of engineering. Among these we can refer to the flow on apartment buildings. In most of the conducted studies only the flow on a barriers inside a canal has been studies and seldom a study has been conducted on two cylindrical. Identification of the physical phenomena of flow on these geometries in Building applications in optimized design has a special importance. Hence, studying flow and Heat Transfer on two barriers inside a canal has attracted the

attention of researchers. The major differences of the present study with that of previous ones are presented below:

In the selected geometry two barriers in the center of canal with fixed temperatures have been studied. This study has been conducted in the lower range of Reynolds number (Reynolds 100 to 300) and the effect of geometrical parameters of the problem on flow field and heat transfer have been studies closely.

1-1- Numerical studies

Young & Vafai [1] have studied forcible convective of flow on a warm barrier with fixed flux which has been located on the wall of a canal at the range of a Reynolds number of 200 to 300. A special emphasis has been placed on calculation of local Nusselt number distribution and average Nusselt number. In this study changes on some barrier parameters such as Width, height and also The thermal conductivity of the fluid to barrier and flow rate have been studied. Results of this study indicate that the shape of the barrier has a great effect on current and heat transfer. Also, with the increase of Reynolds number, average Nusselt number increases. Local distribution of Nusselt numbers also has been obtained on barriers and indicates that Nusselt number increases in the vicinity of the inside corners of flow specially at the upper corner. Rosales et al. [2] in a numerical study has studied the specifications of Unsteady flow and heat transfer for A pair of square cylinder in a calm flow inside a canal. Reynolds number has been assumed to be constant and equal to 500. Drag, lift coefficients and heat transfer have been studied. Results indicate that when the warm barrier approaches the wall, drag coefficient and Nusselt number decrease. Korichi & Oufer [3] have studied Heat transfer displaced between a Newtonian, relaxed and incompressible fluid and three physical barriers located on lower wall (2 barriers) and upper wall (1 barrier) numerically. Walls have been considered as insulator, except for the parts on which barriers are located and beneath barriers constant heat flux is applied. The range of Reynolds number is between 400 to 2000. Effects of changes in Reynolds number, distant and size of barriers as well as thermal conductivity of the solid to liquid ratio have been studied. Results indicate that with increasing Reynolds number, heat transfer from barriers also is also increased that this increase in maximum at the corners of barriers. Tatsutani et al. [4] have studies flow on two square barriers with different heights inside a canal for Reynolds numbers between 200 to 1600 on the basis of downstream length of the barrier. In this study they have found that the special formed patterns in the fluid field depends on the distance between barriers. They have also found that with changing the distant between the barriers, after a critical distance, two vortex are created with different rotation directions between the two barriers. In this case, fluctuations of vortices only have been seen at the downstream of the second barrier.

1-2- Empirical studies

Chen & Wang [5] in an empirical analysis have tested forcible convective currents on two heated barriers on the wall of a canal. This experiment includes mass transfer as well. Based on the similarity of mass transfer and heat transfer, results can be generalized for determining heat transfer as well. The test has been performed for high range of Reynolds numbers. The highest Nusselt numbers has been seen on the initial upper corner on the same direction as of the current. Also, it has been seen that in Turbulent flow with increasing the distance between two barriers, average Nusselt number first reduces and then increases. Sewall et al. [6] have studied flow and heat transfer in a canal with some barriers on walls in high range of Reynolds number. One of the most important aspects studied in this study is flow transfer in the area under development, distribution of average and turbulent quantities in developing, developed areas and bend area.

2- Geometry in this study

Two square warm barriers with constant temperature have been placed insides a canal with Wall insulation. In figure (1) a schematic of the problem and its important parameters have been shown. It should be mentioned that the Coordinates origin on the left wall of the first barrier is located inside the canal and the positive direction of x axis is toward downstream of the flow and the positive direction of y axis is toward upper wall of the canal.

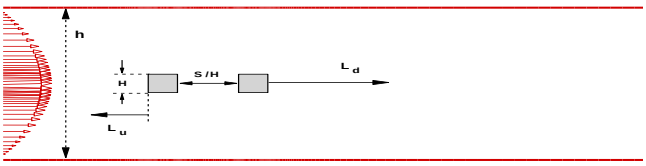

Figure 1: Problem's schematic figure and its important parameters

upwind length (L_u) is equal to 5H and downstream length (L_d) is considered as 24H≥. [7]

S/H: distance ratio between two barriers to height of each barrier and this parameter in this study takes values of 1,2,3 and 4.

B1: Refers to blockage ratio which intern refers to height ratio of each barrier to the widths of the canal (H/h) which is equal to 0.125 in this study.

Reynolds number: (U_{max}.H/ν) which is in the range of 100 to 300.

The used grid in this problem is a Heterogeneous grid which has compaction near canal walls and barriers as well as at the vicinity of barrier corners and with increasing the distant from walls and edges, nodes become looser. Figure (2) presents the grid around the barriers.

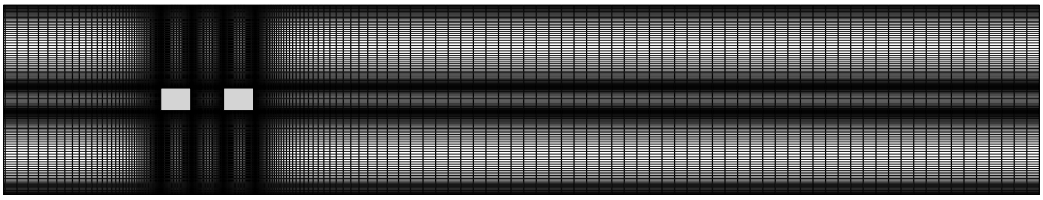

Figure 2: Grid around barriers

One of the analyses which is being performed in numerical problems is the selection of solution grid and independency of solutions from the mentioned network. This discretization is performed in order for us to know eventually that which grid is appropriate for the problem in question. The used method is in this way that first the problem is solved with a rather big grid and in the next stage the grid is made more small and solutions are compared with the previous cases and if the solutions have small difference with each other, the larger grid is selected as the solution network, otherwise making the grid smaller continues until a small difference would be observed between the two final cases of solutions. For studying the effect of changes of the calculated grid and its effect on solutions in the geometries of S/H=2 and Bl=0.5, the sensitivity of solutions to grid size is studies. The smallest size of the grid beside walls respectively has been selected as 0.02H, 0.015H, 0.009 H and 0.007H that the size of grid in them is equal to 231x67, 253x80, 267x93 and 326x125, respectively. Obtained results include Average Nusselt number as well as total drag coefficient which are being compared. From comparing the results obtained from this calculated network, (figure 3), it can be concluded that in Reynolds numbers between 100 to 150 the size of the grid is 0.015 and in Reynolds numbers of 200, 250 and 300 , the grid size of 0.009 is the proper size for the grid.

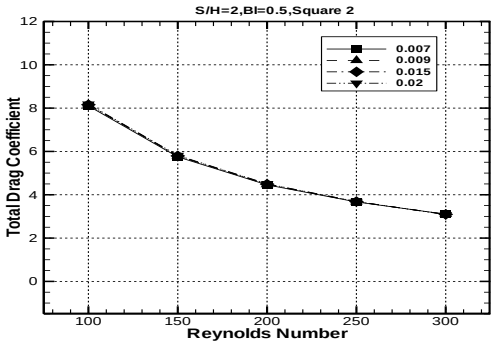

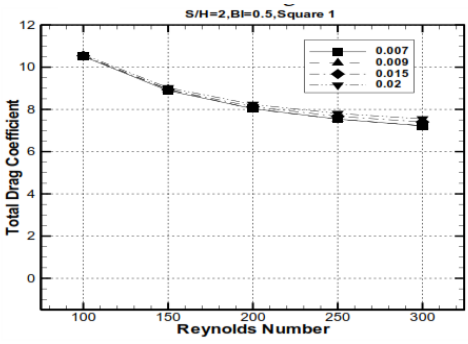

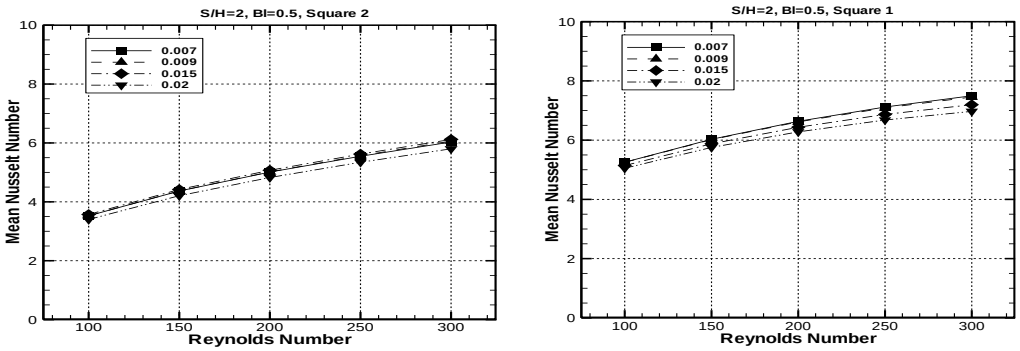

Figure 3: Comparison of the results obtained from calculated grid

2-1- Temporal Convergence

Momentum equations have been considered as transient. In fact, temporal derivatives of speeds have been considered in equations of motion. Sustainable problems also can be solved in transient condition that after some temporal solutions become convergence and final solution is obtained. The point which should be noted is the temporal convergence of solutions, which means that the solving process should be continued until we are confident that the software output is the very sustainable answer or solution. The temporal convergence is selected on the basis that changes become sustainable and show a repetitive process. In some of the studied geometries sustainable conditions have been observe and in another number of them unsustainable conditions have been seen. The averaged value have been selected on the basis of elimination of initial error, approximately 30 first time unit. For answering this problem consider figure (4). In this figure in Reynolds number of 250 in blockage ratio of 0.5 and S/H=2, changes of three points of the field has been drawn with time that the position and location of these three locations and points of the filed have been shown in figure (5).

Figure 4: The location of three points of a, b and c in canal

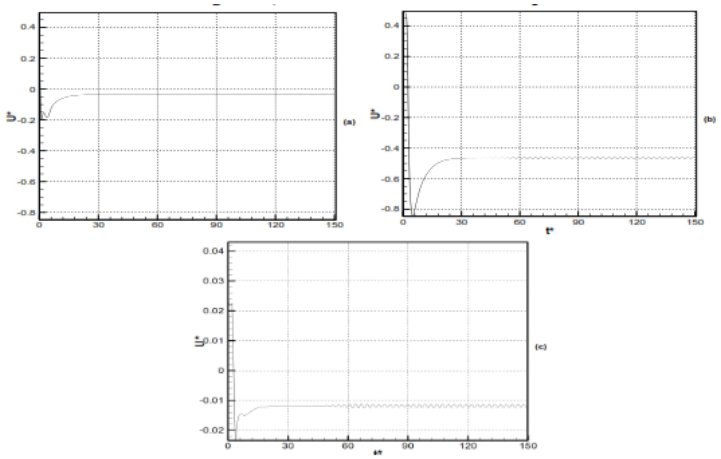

Figure 5: Convergence process of Horizontal component of velocity over time in three points of the field: A) point a, B) point b, C) point c

3- Numerical approach to the problem

Obtained equations from Finite volume method are analyzed and then are solved with the use of new code of UTF [8]. This code has been developed for three-dimensional solution of turbulent follow on complex geometries. In the beginning the way equations have been

analyzed with the use of Finite volume method is explained. This is explained with Spatial discretization for terms of convective , diffusion and time discretization for non-sustainable term and finally fractional step solution for Navier-Stokes equation and direct solution method and for solving linear equations resulted from discretization of the pressure equation (Poisson equation).

3-1- Finite Volume Discretization

Momentum equations in short are presented as below:

$$\frac{\partial \Phi}{\partial t} + \frac{\partial (\Phi U_j)}{\partial x_j} = \frac{\partial}{\partial x_j}\left(\Gamma_\Phi \frac{\partial \Phi}{\partial x_j}\right) + S_\Phi \qquad (1)$$

In which Φ is a function of u, v and w and Γ_Φ ,diffusion coefficient and S_Φ is general source term. Diffusion coefficient and source term have been specified in table (1) according to the equation type.

Table 1: A summary of Diffusion coefficient and source term for The governing equations

Equation	Φ	Γ_Φ	S_Φ
Continuity	1	0	0
Momentum	U_i	υ	$-\frac{1}{p}\frac{\partial p}{\partial x_i}$

The governing equations are analyzed with the use of finite volume method in which the solution area is located inside control volumes. The defined grid inside control volume for Scalar values includes pressure, temperature and so on and control volume of velocity is displaced in a way that Scalar quantities are located in the center of control volume. This change occurs due to separation of the velocity field and pressure which prevents the creation of repetitive state of points. In figure (6), a displaced grid has been shown in 2-D. figure (7) show the three-dimensional control volume on the basis of velocity component of U, the center of which is locate in I, J, K.

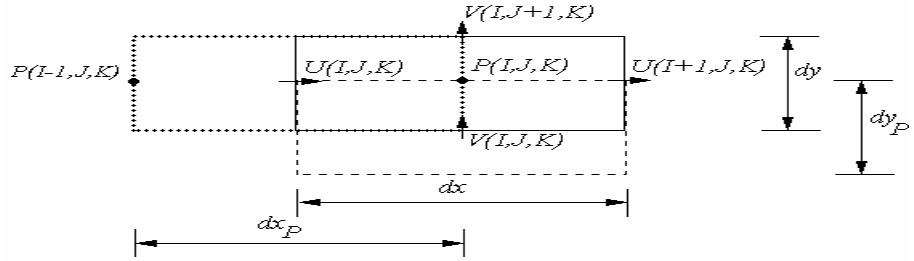

Figure 6: Control volume on a displaced grid for two-dimensional network: continuous lines for control volume of P, dotted line for control volume of U and Non-continuous line for control volume of V

With the integration of equation (1) on each control volume the following equation is obtained.

$$\iiint \left[\frac{\partial \Phi}{\partial t} + \underbrace{\frac{\partial (\Phi U_j)}{\partial x_j} - \frac{\partial}{\partial x_j}\left(\Gamma_\Phi \frac{\partial \Phi}{\partial x_j}\right)}_{F} - S_\Phi \right] dv = 0 \qquad (2)$$

The following equation is obtained with the use of Gauss theorem:

$$\iiint \frac{\partial a_i}{\partial x_j} dv = \iint a_i n_i ds \qquad (3)$$

Volume integral on F term is transferred from equation (2) to Surface integral and the following is obtained from it :

$$\frac{\partial}{\partial t}\iiint \Phi\, dv - \iiint S_\Phi\, dv =$$
$$+ \iint_{east}\left(\Gamma_\Phi \frac{\partial \Phi}{\partial x_j} - \Phi U_j\right) ds_x - \iint_{west}\left(\Gamma_\Phi \frac{\partial \Phi}{\partial x_j} - \Phi U_j\right) ds_x$$
$$+ \iint_{north}\left(\Gamma_\Phi \frac{\partial \Phi}{\partial x_j} - \Phi U_j\right) ds_y - \iint_{south}\left(\Gamma_\Phi \frac{\partial \Phi}{\partial x_j} - \Phi U_j\right) ds_y \quad (4)$$
$$+ \iint_{top}\left(\Gamma_\Phi \frac{\partial \Phi}{\partial x_j} - \Phi U_j\right) ds_z - \iint_{bottom}\left(\Gamma_\Phi \frac{\partial \Phi}{\partial x_j} - \Phi U_j\right) ds_z$$

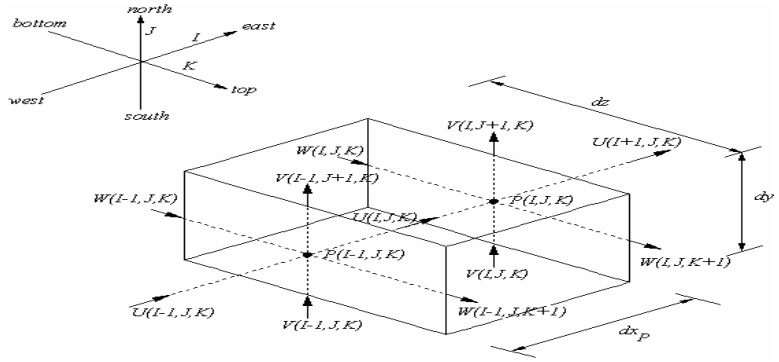

Figure 7: Three-dimensional control volume for U(I,J,K)

Integral on equation (4) is a real integral and for converting it to Algebraic equations we are required to used deferential form and some assumptions for simplifying them. The simplest assumption with the consideration of accuracy of 2nd degree is to show volume integral with the multiplication product of average volume value of $\hat{\Phi}$ in volume.

$$\iiint \Phi\, dv = \hat{\Phi}\, \Delta v \approx \Phi \Delta v \quad (5)$$

The averge volume value of $\hat{\Phi}$ should be calculated from the integral on volume of equation (5). A number of assumptions can be used for obtaining this value. Among these, Interpolation between nodes value or using shape function for example for accuracy of 4th degree, shape function with 4th degree can be named.

In the present study for problem simplification, the existing values in control volume centers as average have been used. According to this assumption all the values on points are available and there is no need for interpolation. This assumption in case of Φ value being constant or in the case it changes linearly inside control volume is equal to the actual value. At the right side of equation (4), Diffusion and convective terms are located which are presented as per the following on control volume surfaces.

$$\iint (Flux)_i\, ds_i = [Flux]_i \Delta s_i \approx Flux\,|_i \Delta s_i \quad (6)$$

For calculating average surface flux in equation (6), [Flux] term, average value of $\Phi, U_j, \frac{\partial \Phi}{\partial x_j}$ on surface Δs_i should be calculated. For determining these values again some assumption have been considered. In the simplest assumption, average of the above mentioned values at the surface center have been considered as average value of total surface. For a full Discretization of the equation, S_Φ value (source term) also should be estimated. From table

(1) it is seen that only for momentum equation the value of source term is not equal to zero and is equal to pressure gradient of $\left(\frac{1}{\rho}\frac{\partial P}{\partial x_i}\right)$.

These two terms in table (2) have been shown in summary and analyzed.

Table 2: Summary of source term in momentum equation

Equation	Φ	$\iiint S_\Phi dv$
Momentum in the direction of x	U	$\iint_{east}\left(\frac{1}{\rho}P\right)ds_x - \iint_{west}\left(\frac{1}{\rho}P\right)ds_x$
Momentum in the direction of y	V	$\iint_{north}\left(\frac{1}{\rho}P\right)ds_y - \iint_{south}\left(\frac{1}{\rho}P\right)ds_y$
Momentum in the direction of z	W	$\iint_{top}\left(\frac{1}{\rho}P\right)ds_z - \iint_{bottom}\left(\frac{1}{\rho}P\right)ds_z$

3-2- Spatial Discretization Scheme

Calculation of average value of source on surface in equation (6-3) includes the production of multiple variables and their gradients on surfaces. ΦU_i is required for convective flux and $\Gamma\left(\frac{\partial U_i}{xj}\right)$ or $\Gamma\left(\frac{\partial T}{x_i}\right)$ is required for Diffusion term. These terms have been calculated with the use of Interpolation of speed, temperature and so on values on points.

3-3- Evaluation of convective flux

Discretization method for convective flux term is so much sensitive and critical in accuracy and sustainability of numerical solution. Values of Φ and U_i in every plate are calculated with the use of one or multiple values from existing points in vicinity of interpolation and convective flux with the use of interpolated values.

A common method for calculation of convective term is discretization of this term into two convective value terms of (Φ) and transfer velocity (U_i). For example, transmission intensity from east plate in control volume of Φ_p shown in figure (3) is expressed as below:

$$[\Phi U]^{east} \approx [\Phi]^{east}_{conv}[U]^{east}_{tran} \qquad [\Phi U_i] \approx [\Phi]_{conv}[U_i]_{tran} \tag{7}$$

Superscript of east (east) is considered as the interpolated value in east plate.

Transfer velocity of $[U]^{east}_{tran}$ has been calculated with the use of linear interpolation of 2nd degree in a non-uniform grid and calculation of convection level of $[\Phi]^{east}_{conv}$ or Φ_e depends on Discretization method.

3-4- Upwind Discretization Scheme

In this method, value of Φ_e is calculated based on upwind or downwind points on the surface of control volume that the selection of upwind or downwind depends on flow movement. This method is equivalent to discretizing 1st order derivative in forward or backward states.

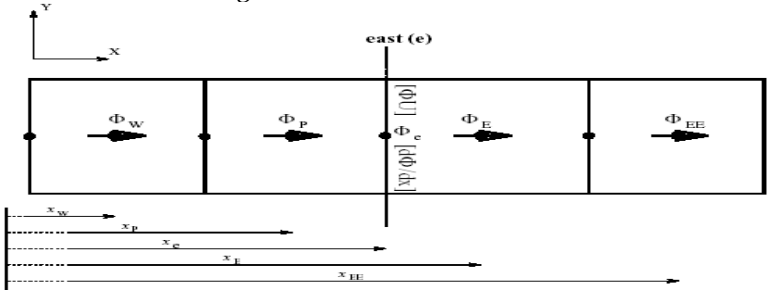

Figure 9: Convective flux and Diffusion on east plats from control volume of P in two-dimensional model

With the use of Taylor expansion between Φ_e and Φ_E , Φ_e and Φ_P we have:

$$\Phi_e = \Phi_p + \underbrace{(x_e - x_P)\left(\frac{\partial \Phi_P}{\partial x}\right)}_{T.E.} + h.o.t. \tag{8}$$

$$\Phi_e = \Phi_E + \underbrace{(x_E - x_P)\left(\frac{\partial \Phi_E}{\partial x}\right)}_{T.E.} + h.o.t. \tag{9}$$

In which h.o.t is error term with a higher rank. The method of UDS has an accuracy of 1st order and error term is proportional to grid distance. In UDS, Φ_e is assumed as per the following.

$$[\Phi]_{conv}^{east} = \Phi_e = \begin{cases} \Phi_E & if \ [U]_{tran}^{east} > 0 \\ \Phi_P & if \ [U]_{tran}^{east} < 0 \end{cases} \tag{10}$$

When the error term is large, this assumption predicts diffusion term as larger and this problems is known as diffusion error [9].

3-5- Linear interpolation

This method is equivalent to central difference scheme (CDS) which is used in finite differential method. This method refers to linear interpolation between two nearer points. In the east plate we will have the following:

$$[\Phi]_{conv}^{east} = \Phi_e \cong \lambda_{e,P}\Phi_E + (1 - \lambda_{e,P})\Phi_P \tag{11}$$

In which $\lambda_{e,P}$ is interpolation coefficient which is equal to $\lambda_{e,P} = \frac{x_e - x_P}{x_E - x_P}$ for a non-unifor grid. This method have a 2nd degree accuracy and its error term is as per the following:

$$T.E. = \frac{(x_e - x_P)(x_E - x_{e)}}{2}\left(\frac{\partial^2 \Phi_P}{\partial x^2}\right) \tag{12}$$

CDS method have numerical dispersion and in case the grid points will not have a proper distance, it is possible that it will convert problem solution to a unsustainable numerical solution. Oscillatory mode will occur if the value of Peclet Number $P_e = \frac{U \Delta x}{\nu}$ would be larger than 2 [9].

3-6- Quadratic Upwind Interpolation for Convective

QUICK model calculates values as per quadratic Upwind Interpolation for convective. This method uses 3 points - 2 points of upwind and a point in downwind of the control volume surface. QUICK relationship for east plate is written as below:

$$[\Phi]_{conv}^{east} = \Phi_e = \begin{cases} g_1\Phi_E - g_2\Phi_W + (1 - g_1 + g_2)\Phi_P & if \ [U]_{tran}^{east} > 0 \\ g_3\Phi_P - g_4\Phi_{EE} + (1 - g_3 + g_4)\Phi_E & if \ [U]_{tran}^{east} < 0 \end{cases} \tag{13}$$

In equation (12), values of g_i are presented as per the following:

$$g_2 = \frac{(1 - \lambda_{e,P})(1 - \lambda_{e,w})^2}{1 + \lambda_{e,P}^2 - \lambda_{e,w}} \qquad g_1 = \frac{(2 - \lambda_{e,w})\lambda_{e,p}^2}{1 + \lambda_{e,P}^2 - \lambda_{e,w}}$$

$$g_4 = \frac{\lambda_{e,P}\lambda_{e,E}^2}{1 + \lambda_{e,E}^2 - \lambda_{e,P}} \tag{14}$$

$$g_3 = \frac{(1 + \lambda_{e,w})(1 - \lambda_{e,P})^2}{1 + \lambda_{e,E}^2 - \lambda_{e,P}}$$

Above equations are correct for uniform and non-uniform grids. Taylor series expansion for Φ_e on a uniform grid with the assumption of $[U]_{tran}^{east}$ is equal to :

$$\Phi_e = \frac{\Phi_P + \Phi_E}{2} - \frac{1}{8}(\Phi_E - 2\Phi_P + \Phi_w) - \underbrace{\frac{3(\Delta x)^3}{48}\left(\frac{\partial^3 \Phi}{\partial x^3}\right)_P}_{T.E.} + h.o.t. \quad (15)$$

That considering equation (12) and with replacement of $g_1 = 3/8$ and $g_2 = -1/8$, the method of QUICK have a 3rd order accuracy. In practice, QUICK method, quantitative value is much more accurate that in linear interpolation. Anyhow, in both the methods, convergence is reached with 2nd order accuracy [10]. Error term is of diffusion material and therefore, has a higher sustainability comparing to linear interpolation.

3-7- Evaluation of the Diffusion Flux

Discretization of diffusion term is based on 2nd order linear interpolation. Calculation of average velocity on the surface or temperature gradient is made with the use of two points and each point is located on the side of the middle point.

Gradient term is expressed as per the following:

$$\left[\frac{\partial \Phi}{\partial x}\right]^{east} = \left(\frac{\partial \Phi}{\partial x}\right)_e = \frac{\Phi_E - \Phi_P}{x_E - x_P} + T.E. \quad (16)$$

Wit considering the above assumption, error term can be written as below:

(16)

$$T.E. = \frac{(x_e - x_P)^2 - (x_E - x_e)^2}{2(x_E - x_P)}\left(\frac{\partial^2 \Phi}{\partial x^2}\right)_e + \frac{(x_e - x_P)^3 - (x_E - x_e)^3}{6(x_E - x_P)}\left(\frac{\partial^3 \Phi}{\partial x^3}\right)_e + h.o.t.$$

This method in uniform grid has a second order accuracy. Error term is proportional with grid points distance and coefficient of expansion in a non-uniform grid [9].

3-8- Temporal Discretization Scheme

Left side of the governing equations include non-permanent term of $(\partial\Phi/\partial t)$. When marching method is used, temporal discretization becomes similar to a spatial Discretization scheme. This non-permanent term shows a specific sharing behavior and spatial terms show a Elliptical behavior.

When a non-permanent term is discretized in relation with spatial fluxes, two groups of methods as explicit and implicit are used. Explicit methods calculate the new value of each point with the use of points' values in pervious temporal steps in new temporal steps directly. Multiple explicit methods have been developed that here in this study Runge-Kutta method has been used. This method is a multiple-points method. In this method, the points between the times t^n and t^{n+1} are used and for starting there is no need of trigger. For defining this method, Nth order equation motioned below is evaluated :

$$\frac{\partial \hat{\Phi}}{\partial t} = F\left(\hat{\Phi}\right) \quad (17)$$

For initial conditions of $\hat{\Phi}^n$ and $F\left(\hat{\Phi}^n\right)$, Nth order Runge-Kutta with temporal step of Δt from $\hat{\Phi}^n$ will be as per the following:

$$\hat{\Phi}^{n+1} = \hat{\Phi}^n + \sum_{j=1}^{N} w_j k_j \quad (18)$$

$$k_j = \Delta t F\left(\hat{\Phi}^n + \sum_{i=1}^{j-1} B_{ji} k_i\right)$$

Degree of Runge-Kutta method shows the accuracy of the method in which W_j term is obtained with the use of the below equation:

$$\sum_{j=1}^{N} w_j = 1 \tag{19}$$

And a constant parameter which is defined as per the following, in which the value of $\mathbf{B}_{ji}$ specifies the method's degree.

$$\sigma_j = \sum_{i=1}^{j-1} B_{ji} \tag{20}$$

3-9- 1st rank Runge-Kutta method (RK1)

In 1st rank Runge-Kutta method with consideration of N=1, equations are reduced to Explicit Euler method with a 1st rank accuracy.

$$\hat{\Phi}^{n+1} - \hat{\Phi}^{n} = F\left(\hat{\Phi}^{n}\right) \tag{21}$$

3-10- 2nd rank Runge-Kutta method (RK2)

In 2nd rank Runge-Kutta first the conditions of $W_1 = 1 - 0.5\sigma_2^{-1}$ and $W_2 = 0.5\sigma_2^{-1}$ should be realized. Considering the fact that the number of unknowns are more than the number of equations (three unknowns and two equations) hence, the problem has more than one solution.

For example,

Developed Euler method $W_1 = 1/2 \ , \quad W_2 = 1/2 \ , \quad \sigma_2 = 1$

$$\hat{\Phi}^{n+1} - \hat{\Phi}^{n} = \frac{\Delta t}{2}\left(F\left(\Phi^{n}\right) + F\left(\Phi^{n} + \Delta t F\left(\Phi^{n}\right)\right)\right) \tag{22}$$

Modified Euler method $W_1 = 0 \ , \quad W_2 = 1 \ , \quad \sigma_2 = 1/2$

$$\hat{\Phi}^{n+1} - \hat{\Phi}^{n} = \Delta t\left(F\left(\Phi^{n}\right) + \frac{\Delta t}{2} F\left(\hat{\Phi}^{n}\right)\right) \tag{23}$$

3-11- 3rd rank Runge-Kutta method

This method of Runge-Kutta has a higher accuracy and comparing to other models with the same accuracy level is more sustainable. The only disadvantage of this method is the storage procedures which are needed for each point in temporal distance (N rank in each temporal step). Low storage of Runge-Kutta similar to 1st rank Euler method requires similar storages and can be developed in any Runge-Kutta method as well. With the proper choice for B_{ij} , σ_j and W_j we will have the following :

$$q_j = a_j q_{j-1} + \Delta t F\left(\Phi^{*}_{j-1}\right) \tag{24}$$

$$\Phi^{*}_{j} = \Phi^{*}_{j-1} + b_j q_j$$

If J=1 , then N and a_1 will be equal to zero. For the case of RK3, $\Phi^{*}_{0} = \hat{\Phi}^{n}$ and $\Phi^{*}_{3} = \hat{\Phi}^{n+1}$ have been shown in figure 10.

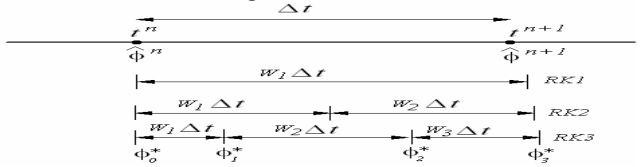

Figure 10: presentation of different Runge-Kutta models with different degrees

Consecutive values of q_i and Φ^{*}_{j} are again written on previous steps. Therefore, in each stage only 2N storage place of q and Φ^{*} is required. Parameters of a_i and b_j can be calculated with the use of replacing the coefficients of σ_j , B_{ij} and W_j .

$$b_j = B_{j+1\ i} \qquad J \neq N$$

$$b_N = W_n$$

$$a_j = \frac{w_{j-1} - b_{j-1}}{w_j} \qquad (j \neq 1,\ W_j \neq 0) \qquad (25)$$

For low storage methods , the required conditions for 3rd rank Runge-Kutta are $w_1 = b_1 + a_2 b_2 + a_2 a_3 b_3$, $w_2 = b_2 + a_3 b_3$ and $w_3 = b_3$. One of the replacement of confidents which satisfies the above conditions is :

$$b_3 = \frac{8}{15} \qquad b_2 = \frac{15}{16} \qquad b_1 = \frac{1}{3} \qquad a_3 = -\frac{153}{28} \qquad a_2 = \frac{5}{9}$$

4- Solution

For solving Navier-Stokes equations, A semi-implicit fractional step is used. Continuity equation and pressure term in momentum equation are expresses in an implicit manner (in new time of t^{n+1}) and diffusion and convection terms in momentum equations are expressed explicitly.

4-1- Semi-Implicit Fractional Step Method

This method is the modified method of stepwise method of Kim and Moin [11]. This method, presents a suggestion based on not using pressure term in prediction of each step which is similar to methods of pressure modification (an algorithm similar to SIMPLE). Pressure in the first step is expresses from the calculation of field explicitly.

In the second step, the used pressure should satisfy continuity law. For a proper presentation of this method, the simplest case of time step of 1st rank Euler in Navier-Stokes equations are evaluated which are shown as Indexes.

$$u_i^{n+1} = u_i^n + \left(SU_i^n + P_i^{n+1}\right)\Delta t \qquad (26)$$

Where, u_i is velocity field; SU_i is the balance of Diffusion and convection terms at every control volume surface; and P_i is pressure term which has been shown implicitly. 1st step: calculation of average velocity field of $u_i^{n+1} = u_i^n + \left(SU_i^n + P_i^{n+1}\right)\Delta t$ from equation (26). 1st and 2nd terms which are at the right side of the equation have been expressed explicitly. In this step, pressure term is disregarded. 2nd step: in this step with the use of continuity equations, a choice is considered implicitly for pressure field. The continuity equations implicitly is expresses in the following way.

$$\frac{\partial u_i^{n+1}}{\partial x_i} = 0 \qquad (27)$$

With replacing u_i^{n+1} from equation (26) in equation (27), Poisson equation is obtained from pressure term. The produced pressure field of P_i^{n+1} in this step is solved with the use of one of the recommended method in the next step. 3rd step: divergence free velocity field of u_i^{n+1} in equation (27) and the obtained pressure in 2nd step. divergence free velocity field has been calculated and now Scalar fields (temperature and so on) in case of necessity can be calculated.

4-2- Solving linear equations

Discretization of pressure term described in 2nd step above causes the occurrence of so many linear equations with the below form.

$$Ax = b \qquad (28)$$

Matrix A is a matrix with low number of members and is a 7 Diagonal matrix nd is the Periodic condition is used, it will become larger. If the used Boundary conditions are appropriate, A will be symmetric with positive eigenvalues. Two different methods, considering the size of A, are used for solving equation (28).

4-2-1 Direct method: LU divisions

Evaluating problems with rather small sizes of memory (usually two-dimensional simulations) are not considered as a serious problem for the memory and therefore, direct method is preferred. In calculation in the present study, LU method has been used. Matrix A with low number of members can be converted into two upper triangle matrix of U and lower triangle matrix of L. the general solution method of these problems are performed with two steps.

1st step: $Ly = b$

2nd step : $Ux = y$

Discretization method of LU is different with Gauss elimination method in which factorization can be performed independently from b. in direct method, however, storage of all the elements of matrix is necessary. For solving problems with so many number of points, a large memory is needed and therefore, Iterative procedure is evaluated.

4-2-2 Iterative procedure: Conjugate Gradient Method

With the use of Iterative procedure, matrix A is converted into two matrix in a way that A=M-N, in this way equation (28) is converted into the following equation.

$$Mx = Nx + b \tag{29}$$

Repeating K+1:

$$Mx_{k+1} = Nx_k + b \tag{30}$$

Error level in each Iterative is equal to:

$$r_k = b - Ax_k \tag{31}$$

The obtained results, after specified iteration has a smaller error level than the allowable limit, error level with the use of equation (31) and reducing Mx_k from its both sides is equal to the following:

$$r_k = M\delta_k,\ \delta_k = x_{k+1} - x_k \tag{32}$$

Iterative procedure is effective when convergence action occurs fast. This indicate the fact that Iterative matrix of M is a well-condition matrix. Considering the characteristics of the matrices, the use of conjugate gradient method can be one of the best options. On the other hand, with the use of some of the Preconditions also the speed of convergence can be increased.

Limitation of conjugate gradient is in that matrix A should be a symmetric matrix and should have positive and known eigenvalues. The main idea in this method is to convert equation (28) into a minimum problem. Error level (r) has minimized and is expressed as a gradient term of the minimum function. With the use of path function search, minimizing process directs us toward the right side of the equation.

Conjugate gradient algorithm is only recommended for calculations related to Scalar values and vector values matrix. Convergence criterion in this method is based on error value average or maximum iterative value (K_{max}). In any case, convergence process is so much slow and this is due to the fact that matrix A is not well-conditioned. The number of iterative number can be considered equal to the number of grid points but this recommendations is not that much acceptable in practice. Convergence percentage of conjugate gradient method is measured based on the distribution of eigenvalues of Matrix A. Hence, it appears that producing a precondition is necessary for increasing the speed of convergence. This is achieved with the use of the precondition of C which is multiplied to both sides of equation (28) *($C^{-1} Ax = C^{-1}b$).* Matrix C should be a known and positive symmetric matrix and should be selected in a way that matrix $C^{-1}A$ would be a well-conditioned matrix or will have a desirable spectrum of known values of matrix A. In case matrix C is a symmetric matrix, the following can be shown:

$$C = KK^t \quad , K \in \Re$$

The method of conjugate gradient precondition is equivalent with normal conjugate gradient method which is expressed in the following way.

$$\underbrace{K^{-1}AK^{-t}}_{\tilde{A}}\underbrace{K^{t}x}_{\tilde{x}} = \underbrace{K^{-1}b}_{\tilde{b}} \qquad (34)$$

Selecting a good precondition can have a considerable effect on convergence procedure and time of CPU. Numerical calculation indicate that in so many cases using Incomplete Chollesky factorization matrix (IC) from matrix A can be a good choice for matrix C, with modification of this method, factorization method of other forms of preconditions such as MICo, IC3, ICo and MIC3 also have been used.

5- Results

5-1 evaluating solutions with previous works

In this study first for evaluating the accuracy of the obtained solutions, heat transfer flow on a square barrier inside a canal has been studies that the obtained Strouhal Number has been compared with the results presented by Breuer et al. [12], Suzuki et al. [13], Guo et al. [14] and Amit Agrawal et al. [15]. As it has been shown in figure (11), obtained results in this study have an acceptable accuracy comparing to previous works.

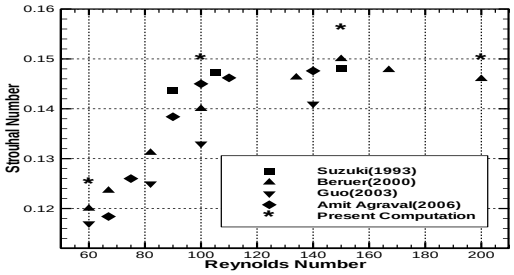

Figure 11: Changes curve of Strouhal number in flow on a square barrier inside a canal

5-2- Change of local Nusselt

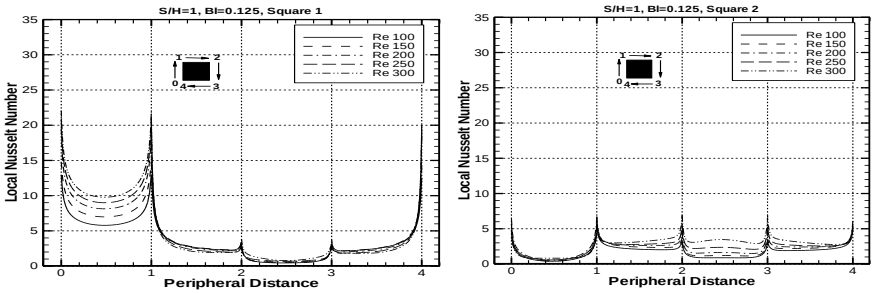

Figure 12: Changes in local number with different Reynolds numbers A) 1st barrier, B) 2nd barrier for S/H=1

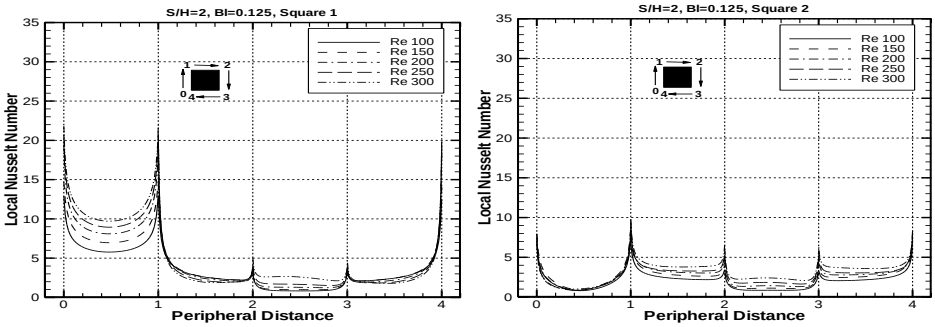

Figure 13: Changes of local Nusselt with different Reynolds numbers A) 1st barrier, B) 2nd barrier for S/H=2

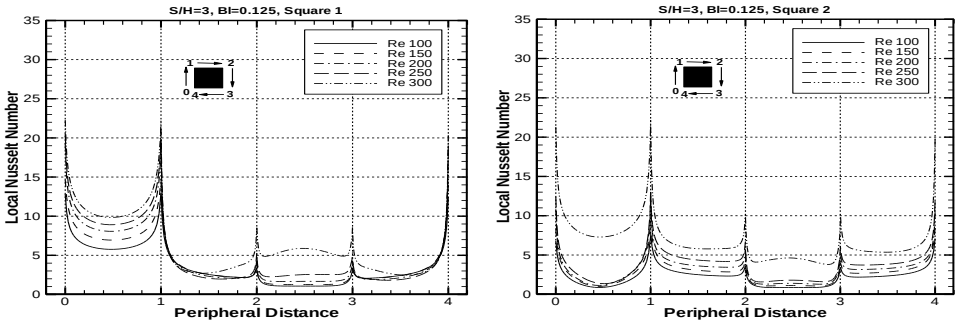

Figure 14 : Changes of local Nusselt with different Reynolds numbers A) 1st barrier, B) 2nd barrier for S/H=3

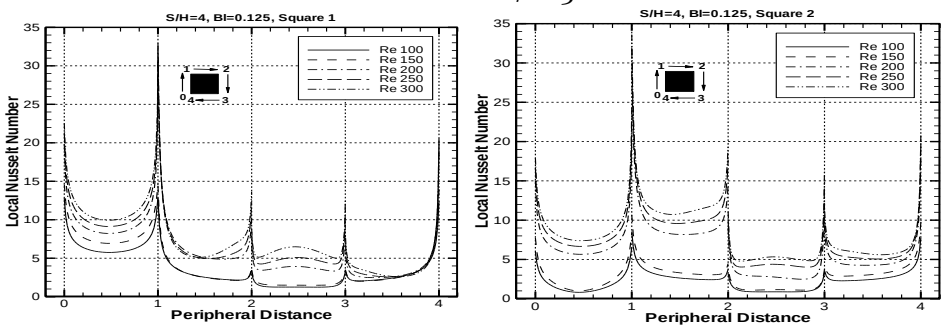

Figure 15: Changes of local Nusselt with different Reynolds numbers A) 1st barrier, B) 2nd barrier for S/H=4

5-3- Evaluating changes of average Nusselt in different S/H and in different Reynolds

Figure (16) in a way has categorized the results and since the relevant descriptions and explanations have been presented earlier, here only results have been presented.

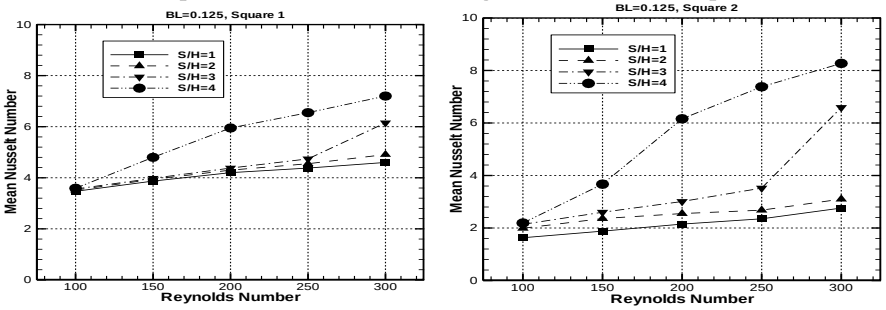

Figure 16: Changes of average Nusselt in different Reynolds and different S/Hs A) 1st barrier and B)2nd barrier

5-4- Studying drag coefficient in different S/H s and in different Reynolds

Figure (17) presents a classiviaotn of results in a different way.

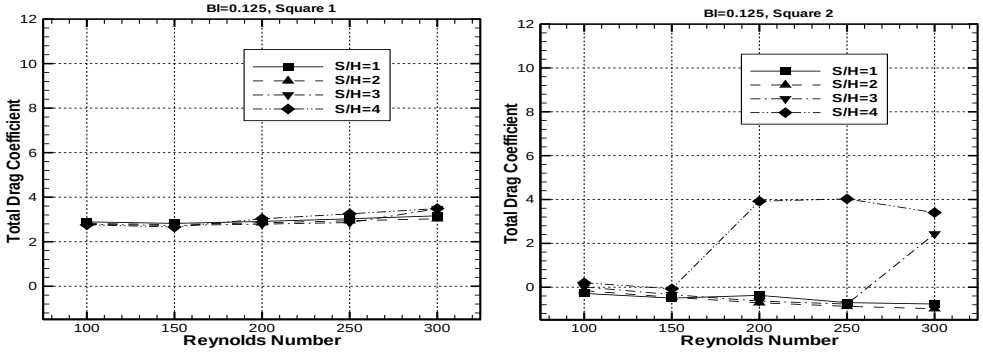

Figure 17: Changes in total drag coefficient in different Reynolds and in different S/Hs A) 1st barrier, B) 2nd barrier

5-5- The relation of average Nusselt with Reynolds number n different arrangements:
After evaluating Nusselt number in different arrangement and considering the curve changes in different Reynolds numbers, mathematical relationship for evaluating changes of Nusslet number with Reynolds numbers in different arrangements are presented in table (3):

$$\overline{Nu} = a\,\mathrm{Re}^{\,b} \qquad (35)$$

Table 3: Relationship of average Nusselt number with Reynolds number

	1st barrier		2nd barrier	
S/H	a	b	a	b
1	1.07	0.2564	0.187	0.4644
2	0.8957	0.2964	0.3622	0.3705
3	0.4361	0.4456	0.0329	0.8813
3	0.1945	0.6378	0.0068	1.2615

6- General results
The important thing in Reynolds' increase, as per figure (18) is the change of the shape of flow lines. In S/H=1 , with increwsing Reynolds number, Vortices move on the Lateral surface of the barriers and the length of vortex behind 2nd barrier increases with the increase of Reynolds number and then reduces. In S/H=2, something totally similar to S/H=1 occurs, the only difference is that increased distance between the barriers causes the movement of vortices to occur on barriers on higher Reynolds and this phenomenon leads to a delay in the reduction of vortex length behind the 2nd barriers with increased Reynolds.
In S/H=3, with an increase in Reynolds number, vortices behind the 1st barrier start to move of upper and lower faces of barriers that eventually at Reynolds of 300 the vortex behind the 1st barrier no more fills the space between the two barriers. Considering the mentioned occurrences in this arrangement, the length of the vortex behind the 2nd barrier first increases and then reduces. In S/H=4 also, increased Reynolds number leads to the movement of vortices between the two barriers on barriers' faces, however, with the start of the movement of vortices on barriers' faces and the increase of Reynolds number, in Reynolds of 200, the vortex behind the 1st barrier no more fills the space between the two barriers and this causes a reduction in the length of the vortex behind the 2nd barrier until it reaches a Reynolds number of 200 and then increases the length of the vortex after this Reynolds number.

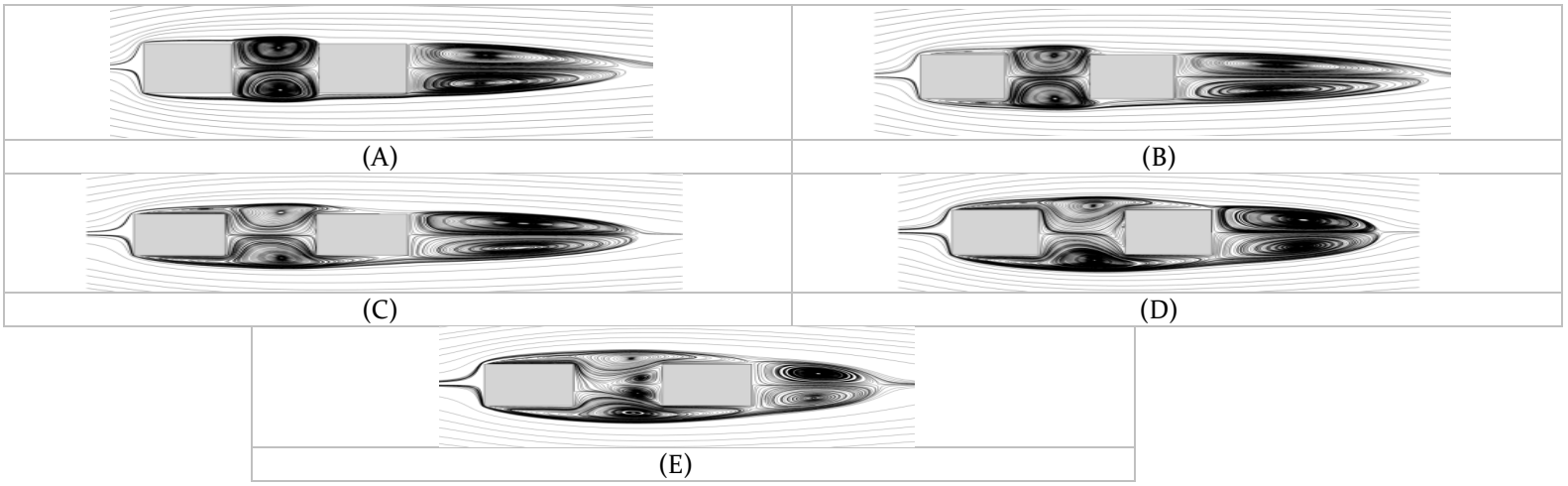

Figure 18: average time of flow lines in S/H=1 A) Re=100, B, Re=150, C) Re=200, D) Re=250 and E) Re=300

6-1- Effect of Reynolds' change on total drag coefficient of the barriers

Increased Reynolds for the 1st barrier in all the S/Hs leads to an increases drag coefficient, however, for the 2nd barrier and in S/H=1 and S/H=2 drag coefficient reduces. In S/H=3 and S/H=4, considering the change in the flow shape and the fact that the space between the two barriers is not filled by vortices, up to the Reynolds number in which the distance between the barriers have been filled with vortices, drag coefficient reduces and after that it increases. This critical Reynolds number in S/H=3 is 250 and it is 150 in S/H=4.

6-2- The effect of Reynolds change in average Nusselt of the barriers

On both of the barriers located inside the canal, increased Reynolds leads to an increase in average Nusselt.

6-3- Effect of distance change between barriers on total drag coefficient of barriers

For the 1st barrier, increased distance between barriers in all the Reynolds numbers, don't have a significant change on drag coefficient. For the second barrier, until the time that the vortex behind the 1st barrier fills the gap between the two barriers, changes in drag coefficient are practically negligible, however with the change of flow arrangement, drag coefficient increases.

6-4- Effect of change of distance between the barriers on average Nusselt of the barriers

With an increase in the distance between the barriers for the 1st barrier, average Nusselt increases, however, increased Reynolds have a direct effect on increased average Nusselt in different distances of barriers. The highest level of average Nusselt jump in defend Reynolds is at the barriers distance between 3H and 4H which is due to the effect of Vortex shedding phenomenon in heat transfer. On the 2nd barrier also, increased distance between the barriers also in general leads to increased average Nusselt, in which Reynolds number has a direct relationship with x average Nusslet's increase.

References

1. T. J. Young, K. Vafai, Convective cooling of a heated obstacle in a channel, *International Journal of Heat and Mass Transfer* 41 (1998) 3131-3148.
2. J.L.Rosales, A. Ortega and J.A.C.Humphrey, A numerical simulation of the convective heat transfer in confined channel flow past square cylinders: comparison of inline and offset tandem pairs, *International Journal of Heat and Mass Transfer* 44 (2001) 587-603.
3. A. Korichi, L. Oufer, Numerical heat transfer in a rectangular channel with mounted obstacles on upper and lower walls, *International Journal of Thermal sciences* 44 (2005) 644-655.
4. R. Tatsutani, R. Devarakonda and J.A.C. Humphrey, Unsteady flow and heat transfer for cylinder pairs in a channel, *International Journal of Heat and Mass Transfer*, Vol. 36, pp. 3311-3328, 1993.
5. Y. M. Chen, K. C. Wang, Experimental study on the forced convective flow in a channel with heated blocks in tandem, *Experimental Thermal and Fluid Science* 16 (1998) 286-298.
6. E. A. Sewall, D. K. Tafti, A. B. Graham and K. A.Thole, Experimental validation of large eddy simulations of flow and heat transfer in a stationary ribbed duct, *International Journal of heat and fluid flow* 27 (2006) 243-258.
7. Sohankar.A, Norberg.C and Davidson.L,, Low-Reynolds flow around a square cylinder at incidence:study of blockage, onset of vortex shedding and outlet boundary condition, Int.J. Numerical method in fluids, Vol.26, 39-56, 1998.
8. A. Suksangpanomrung, Investigation of Unsteady Separated Flow and Heat Transfer Using Direct and Large Eddy Simulations, PhD thesis of Victoria University, Canada, 1999.
9. J.H.Ferziger, M. Peric, Computational Methods for Fluid Dynamics, 2nd E.D., Springer, 1999.
10. B. P. Leonard, Order of Accuracy of QUICK and Related Convection-Diffusion Schemes, NASA Technical Memorandum 106402. Technical report, Institute for Computational Mechanics in Propulsion, Lewis Research Center, Ohio, USA, 1993.
11. J. Kim, P. Moin, Application of a Fractional-Step Methods to Incompressible Navier-Stokes Equations, Journal of Computational Physics, Vol. 59, 1985, pp. 308-323.
12. Breuer, M., Bernsdorf, J., Zeiser, T., Durst, F., "Accurate computations of the laminar flow past square cylinder based on two different methods: lattice-Boltzman and finite volume," Inter. J. Heat Fluid Flow, Vol. 21, pp 186–196, 2000.
13. Suzuki H, Inoue Y, Nishimura T, Fukutani F, Suzuki K. Unsteady flow in a channel obstructed by a square rod (crisscross motion of vortex). Int J Heat Fluid Flow 1993; 14:2–9 .
14. Guo WB, Wang NC, Shi BC, Guo ZL. , Lattice-BGK simulation of a two-dimensional channel flow around a square cylinder. Chinese Phys 2003; 12:67–74 .
15. Amit Agrawal a, Lyazid Djenidi b, R.A. Antonia, Investigation of flow around a pair of side-by-side square cylinders using the lattice Boltzmann method, Computers *&* *Fluids* 35 (2006) 1093–1107 .